Collisional depopulation of Rydberg P states of rubidium at thermal energies

F. Gounand, P. R. Fournier, and J. Berlande
Centre d'Etudes Nucléaires de Saclay, Service de Physique Atomique, B.P. 2-91190, Gif-sur-Yvette, France
(Received 12 November 1976)

We have measured total cross sections for the collisional depopulation of high-lying nP states ($12 \leq n \leq 22$) of rubidium induced by thermal collisions with ground-state rubidium or rare-gas atoms. It is observed that for $n \geq 14$ the rubidium–rare-gas cross sections do not vary with the principal quantum number, contrary to previous hypotheses. Our results are discussed using the simple argument of quasifree behavior of the valence electron involving either an elastic-scattering or a binary-encounter approach. However, the disagreement observed between the experimental and the computed cross sections suggests that a three-body approach is generally needed for a good understanding of collisional processes involving highly excited states.

I. INTRODUCTION

The interest in studying the collisional properties of Rydberg states has been clearly pointed out by recent experimental[1-3] and theoretical[4-6] works. In a previous Letter[3] concerning the total collisional depopulation of a high-lying P state of potassium due to a perturbing gas (potassium or rare-gas atom in its ground state), we have shown that the quenching cross-section values vary, as a function of the nature of the perturber, as the corresponding electron-atom elastic scattering cross-section values. To study this similarity in more detail and to obtain more information on the collisional processes involving Rydberg states, we began a study of the collisional quenching, at thermal energies of highly excited P states of rubidium atoms as a function of both the binding energy of the valence electron and the nature of the perturbing atom (rubidium or rare-gas atom in its ground state). These states are created in a rubidium vapor by photoexcitation from the 5S ground state. We have chosen rubidium because the oscillator strengths of the $5S$-nP transitions are much larger than the corresponding ones in the case of potassium, thus making possible such measurements with a high sensitivity.

Various collisional mechanisms lead to the depopulation of a given highly excited level: excitation transfer to a neighboring level, direct or associative ionization, etc. To our knowledge no data concerning the quenching of highly excited levels are available. Such data are of great practical interest in numerous areas (astrophysics, ionized gases). Moreover, they permit the evaluation of the importance of the collisional effects in experiments dealing with other properties of Rydberg levels (lifetime or fine-structure measurements, for example). Finally, the quenching-rate coefficients are essential parameters in the analysis of experimental data concerning a particular collisional process (electronic excitation transfer, for example). The quenching cross-section values, which are upper limits for the cross-section values associated with particular inelastic channels, and their behavior as a function of the main parameters of the collision (binding energy of the outer electron, nature of the perturbing gas) provide, as we will see, a most interesting check of the available theoretical approaches.

II. EXPERIMENTAL SET-UP

We have measured the total quenching cross section corresponding to the process:

$$\mathrm{Rb}(nP) + X \xrightarrow{Q_X(nP)} \mathrm{Rb}(\neq nP) + X\,, \tag{1}$$

where Rb(nP) is a rubidium atom excited to the nP state; X, either a rubidium ground state (Rb) or rare-gas (G) atom; $Q_X(nP)$, the quenching cross section of the nP level; and Rb ($\neq nP$), a rubidium atom excited to a state (neutral or ionic) different from the initial one. The quenching cross section $Q_X(nP)$ is defined, as usual in a gas-cell experiment, from the relation

$$K_X^Q(nP) = Q_X(nP)\bar{v}_{\mathrm{Rb}\text{-}X}\,, \tag{2}$$

where $K_X^Q(nP)$ is the rate constant for reaction (1), and $\bar{v}_{\mathrm{Rb}\text{-}X}$ is the Maxwellian-averaged relative velocity of the two colliding atoms. The values of the $K_X^Q(nP)$ rate constants are deduced (see Sec. III A) from the measurement of the effective lifetime of the nP level as a function of the density of the perturbing atom.

The experimental set-up is shown in Fig. 1. A nitrogen laser (Molectron UV 1000), and a Rhodamine B dye laser, followed by an extra-cavity frequency doubling device using a KDP crystal produce the uv pulses ($\lambda \sim 3000$ Å). These pulses have an average duration of about 3 nsec, with an energy of 10^{-5} J per pulse and a linewidth of 0.3 Å. The repetition rate can be varied up to 30 Hz. The uv

power is high enough to insure a noticeable population of some highly excited P states of rubidium. The uv beam passes through the experimental cell containing rubidium vapor. This cell is set in an oven maintained at a fixed temperature ($T = 460°K$). The liquid rubidium is located in a sidearm, the temperature of which can be kept at a fixed value (over the range 330–400 °K) by a separate heating system. Thermocouples provide the measurement and the regulation of the temperature in the whole system. The measurement cell is connected by a capillary to a vacuum or gas filling system. After a typical baking procedure the residual pressure is about 5×10^{-7} Torr. The rare-gas pressure, ranging from 2×10^{-3} to a few Torr, is measured with an oil-manometer and the rubidium vapor pressure, ranging from 8×10^{-6} to 5×10^{-4} Torr, is determined by the temperature of the sidearm containing liquid rubidium.[7] The fluorescence light is analyzed with a grating monochromator which selects a line originating from the pumped level (we observe the $nP \rightarrow 4D$ transition in the 7000–7600-Å range). The lifetime measurements are then made by using a high-speed cooled photomultiplier (C 31034 type), a 100-MHz counting system (amplifier and discriminator) and a twenty channel scaler connected to a PDP 15 computer. The channel width can be varied from 40 nsec up to several μsec according to the experimental requirements. A trigger system starts the analysis a short time (~15 nsec) after the laser pulse.

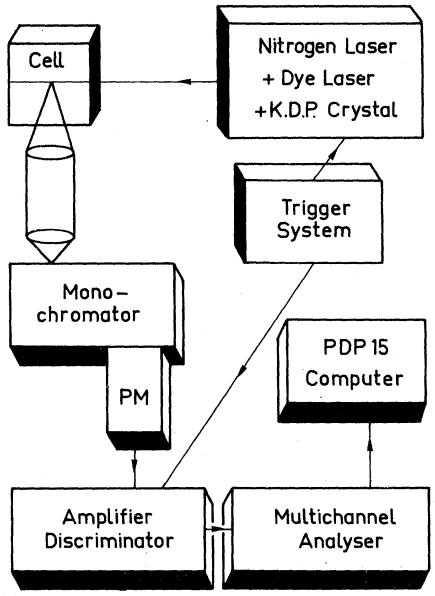

FIG. 1. Schematic diagram of the apparatus.

III. DATA ANALYSIS

A. Decay frequency determinations

As mentioned previously, the quenching cross-sections were obtained by measuring the effective lifetime of the nP excited level as a function of the density of the perturbing gas. We can write

$$\frac{1}{\tau} = \frac{1}{\tau_{\text{rad}}} + \frac{1}{\tau_{\text{Rb}}} + \frac{1}{\tau_G}, \tag{3}$$

where τ is the measured lifetime and τ_{rad} the radiative lifetime ($1/\tau_{\text{rad}} = \sum_i A_i$ where the A_i's are the Einstein coefficients of all the lines originating from the nP level). The last two terms on the right side of Eq. (3) represent the effect of collisions with rubidium and rare-gas atoms, respectively, on the lifetime. These terms can be written as

$$\begin{aligned} 1/\tau_{\text{Rb}} &= N_{\text{Rb}} Q_{\text{Rb}}(nP) \bar{v}_{\text{Rb-Rb}}, \\ 1/\tau_G &= N_G Q_G(nP) \bar{v}_{\text{Rb-}G}, \end{aligned} \tag{4}$$

where N_{Rb} and N_G are the rubidium and rare-gas densities; $\bar{v}_{\text{Rb-Rb}}$ and $\bar{v}_{\text{Rb-}G}$ are the Maxwellian averaged velocities of the relative motion of the two colliding atoms for the (Rb-Rb) and (Rb-G) collisions, respectively. Equation (4) implies that other atomic levels do not contribute radiatively or collisionally to the population of the considered nP level, that is to say no "repopulation" of the nP level is present (when originating from more highly excited level this repopulation is also called cascading).

Equations (3) and (4) show that the variation of $1/\tau$ as a function of N_{Rb} (with $N_G = 0$) is linear with a slope proportional to $Q_{\text{Rb}}(nP)$. Similarly, the variation of $1/\tau$ as a function of N_G (with $N_{\text{Rb}} = Ct$) allows the determination of $Q_G(nP)$. Moreover, the extrapolation of the $1/\tau$ value to zero rubidium pressure yields the natural radiative lifetime of the considered level. Results concerning the τ_{rad} values are published elsewhere.[8] They range from 1.55 μsec for $n = 12$ to 14 μsec for $n = 22$. Repopulation effects can be seen in Fig. 2, which shows semi-log plots of the population decay of the $22P$ level for two different time scales. The linear decay of log (I_t) seen at early times (curve A) indicates that repopulation effects are almost negligible during that time. At late times (curve B) the effect of repopulation of the level becomes apparent. This is in accordance with the well-known fact that, in a first approximation, repopulation effects become noticeable after a time on the order of the effective lifetime of the repopulating level. For the rare gas the lowest pressure investigated was 2×10^{-3} Torr. At this pressure no departure from the decay obtained for zero rare-gas pressure was observed in the case of the three gases investigated here. Then the rare-gas pressure was increased by small amounts in order to follow

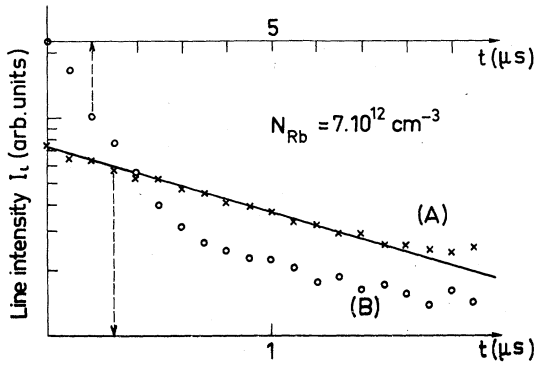

FIG. 2. Experimental decay curves observed for the 22 P state in rubidium (perturber: ground-state rubidium). Points (A) refer to the lower scale, points (B) to the upper scale.

accurately the τ variation and to detect any anomalous behavior. For the measurement of $Q_G(nP)$ we chose the lowest possible rubidium pressure and verified that a significant change in the rubidium pressure did not affect the value of $Q_G(nP)$. Finally, the slope of the curves (i.e., see Fig. 3) determining $Q_{Rb}(nP)$ and $Q_G(nP)$ were obtained from a classical least-square fitting procedure.

B. Uncertainties

1. Negligible effects

We would like first to discuss the influence on the measured lifetime of impurity gases which may be present in the cell or in the rare gas.

The average background pressure in the cell is 5×10^{-7} Torr, as indicated previously. When only rubidium vapor is present, collisions between excited rubidium atoms and impurities would add a constant term $[1/\tau_{imp}=N_{imp}\bar{v}Q_{imp}(nP)]$ to the right side of Eq. (3) and therefore affect the measured $1/\tau_{rad}$ at very low rubidium pressures. Experimentally it is observed[8] that the measured values of $1/\tau_{rad}$ do not exhibit a constant deviation from the corresponding theoretical values.[9] Moreover the variation of the τ_{rad} as a function of the effective quantum number n^* is in good agreement with the theoretical prediction of the quantum defect theory (i.e., $\tau_{rad}\sim n^{*3}$). Finally, during one set of measurements, a small leak in the vacuum system gave rise to an increase in the background pressure to 10^{-5} Torr. Such an increase reduced the observed τ of the 17P level by 30% for a rubidium pressure of 8×10^{-6} Torr. From this observation one can estimate the quenching cross sections for the residual impurities to be on the order of 4×10^{-12} cm^2. This indicates that for a residual pressure of 5×10^{-7} Torr the τ measured for very low rubidium pressure would be affected by less than 3% for the 22P level and much less for the other levels. But it does not affect the values of $Q_{Rb}(nP)$ which are deduced from the slopes of the $1/\tau=f(N_{Rb})$ curves (since the background pressure would be only adding a constant value to the observed $1/\tau$ decay).

The concentration of the molecular impurities in the rare gas used (Gaz Industriels de la Courneuve) is less than 7 ppm for neon and argon and less than 3 ppm for helium. In view of the quenching cross sections measured for the rare gases only residual impurities having quenching cross sections on the order of 10^{-10} cm^2 could affect the results of this work. Such cross sections look most improbable and are well above the previously deduced value (4×10^{-12} cm^2). Before its introduction into the measuring cell the rare gas is stored at a pressure of about 500 Torr in a tank where a residual vacuum of 5×10^{-7} Torr was obtained. Therefore a negligible pollution of the rare-gas occurs before it is introduced in the cell.

We are led to conclude that under our experimental conditions impurity gases do not affect significantly the measurements.

The $nP\rightarrow4D$ fluorescence emissions, used to monitor the population decay of the nP levels, are not trapped because their terminal state is not the ground state.

The determination of $1/\tau_{Rb}$ from the difference between the measured $1/\tau$ and $1/\tau_{rad}$ [see Eq. (3)] was done assuming that $1/\tau_{rad}$ does not change when varying the rubidium pressure. It is easy to show that this introduces a negligible error in view of the magnitude of the trapping effect. Only the $nP\rightarrow5S$ transitions are trapped. In the most unfavorable case (12$P\rightarrow5S$ transition) the optical path in the cell (~0.5 cm) is much smaller than the absorption length (25 cm, assuming $A_{12P\rightarrow5S}=6.5\times10^4$ sec^{-1}, for the highest rubidium density investi-

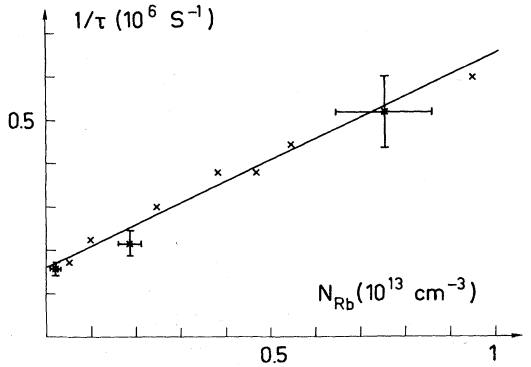

FIG. 3. Plot of the inverse of the experimental effective lifetime vs rubidium pressure for the 17P level in rubidium.

gated i.e., ~10^{13} cm^{-3}). Moreover this transition contributes only for 15% to the spontaneous emission rate $\sum_i A_i$ of the 12P level.[9] Therefore the maximum error due to trapping when varying the rubidium density is less than 0.3% of the $1/\tau_{rad}$ for the 12P level.

Only one maximum in the fluorescence intensity is observed when the laser wavelength is swept across the absorption line. We measured the lifetime as a function of the laser wavelength across the absorption line for the 12P level, whose fine-structure interval between the $^2P_{1/2}$ and $^2P_{3/2}$ sublevels is on the order of the laser linewidth, and no systematic variation was observed, within experimental error. Thus we consider that the $n^2P_{1/2}$ and $n^2P_{3/2}$ sublevels are both involved in this experiment.

The uv light from the laser exhibits a high degree of linear polarization. The experimental observation were made at a right angle to the uv beam with a detection system insensitive to polarization. By using the multipole expansion of the time dependence of the fluorescence light, one can show that the well-known effects of polarization[10] are not important under the present experimental conditions. This was also deduced from the experimental curves obtained.

Although a recent work[11] indicates the possible existence of cooperative effects when the laser power is high enough, such effects should not be expected for the present experimental conditions. This was confirmed by measuring the lifetime τ for different energies of the exciting beam (attenuating the beam by a factor up to 20) and observing no systematic variation.

During a typical lifetime τ the excited atoms can travel over distances on the order of some millimeters. This may introduce a systematic error in the measurement of τ, if the atoms escape from the observed volume before radiating. If this is the case a corrective term has to be added to the right side of Eq. (3). In order to reduce any such effect, we used an exciting beam whose dimensions (~15×7 mm) were much larger than those of the volume observed by the optical detection system. An almost homogenous population density of excited species is thus insured in the observed volume. We estimate that the resulting error for the largest measured lifetimes (~7 μsec) would not exceed 10%.

2. *Experimental errors*

The experimental errors associated with the measured values of $Q_X(nP)$ come mainly from the accuracy on the $1/\tau$ values (coming from counting errors) and from the determination of N_{Rb} and N_G. The uncertainty associated with the counting rate is between ±3 and ±11%, taking into account the dead time of the counting apparatus and the statistical error. The calibration of the time scale of the 20 channel scaler is made with an accuracy of ±1%. Thus one can consider that the determination of a lifetime τ value [deduced from the $\log(I_t)=f(t)$ curve] is achieved with better than ±12% accuracy [the relative error on the $\log(I_t)$ values being smaller than 11% in view of the obtained counting rates]. The determination of the rare gas pressure is made with an accuracy of better than ±5% for $P_G \geq 10^{-2}$ Torr. The thermal transpiration correction (the oil-manometer not being at the same temperature as the measurement cell) is sufficiently accurate to allow finally the determination of N_G in the measurement cell with better than ±8% uncertainty. We can thus estimate the accuracy of the $Q_G(nP)$ values to be about ±20% in the worst cases.

The rubidium density is derived from the temperature of the sidearm containing liquid rubidium. Gallagher and Lewis[12] have shown that with proper experimental care, such a determination can be trusted in the lowest range investigated here (~10^{-5} Torr). Precautions similar to those reported in Ref. 12 were taken to insure that the results are independent of the temperature history of the measuring cell. Moreover we verified that the density measurements agreed within ±15% with those determined from absorption measurements of the resonance line for vapor pressures greater than 6×10^{-5} Torr (the pressure range in the experiment was 8×10^{-6} to 5×10^{-4} Torr). Our apparatus is not sensitive enough to allow measurements below this pressure. However, the τ_{rad} values, as obtained by the extrapolation of $1/\tau$ values (measured for $8\times10^{-6} \leq P_{Rb} \leq 5\times10^{-4}$ Torr) do not exhibit any anomalous behavior, as pointed out previously. In conclusion we estimate that the determination of N_{Rb} is achieved with better than ±25% accuracy (including both the deviation between the absorption measurements and the calculated vapor pressure (±15%), and an estimated confidence limit of 10% for the vapor pressure curve), giving rise to a total uncertainty of ±37% for the $Q_{Rb}(nP)$ values in the worst cases.

IV. RESULTS AND DISCUSSION

Table I shows our experimental results. We have chosen to consider exclusively the $n=12$, 14, 17, and 22 levels whose ionization energies scale down smoothly. This permits the extension of our previous work[3] towards more highly excited levels while keeping a reasonable data collection time (although this is no longer the case for $n>22$). The following points can be noted from Table I.

TABLE I. Quenching cross sections $Q_X(nP)$ for nP states in rubidium. All the cross sections are in Å^2. E_i is the ionization energy of the considered level.

Level	E_i (eV)	n^4	Perturber X Rb	He	Ne	Ar
$12P$	0.19	2.1×10^4	$(2.3\pm0.8)\times10^3$	38 ± 7	4.9 ± 0.9	15 ± 3
$14P$	0.11	3.8×10^4	$(7.1\pm2.5)\times10^3$	56 ± 10	12 ± 2.4	25 ± 5
$17P$	0.066	8.3×10^4	$(1.00\pm0.35)\times10^4$	58 ± 11	11 ± 2.1	28 ± 5
$22P$	0.036	2.3×10^5	$(1.6\pm0.6)\times10^4$	60 ± 12	13 ± 2.5	30 ± 6

(i) The $Q_{Rb}(nP)$ cross-section values are about two orders of magnitude larger than the corresponding $Q_G(nP)$ values.

(ii) The behavior of the $Q_{Rb}(nP)$ values as a function of n is different from the corresponding behavior of the $Q_G(nP)$ values. A significant increase is observed in $Q_{Rb}(nP)$ with n that is not directly related to the geometrical size of the excited atom, i.e., $\sim n^4$. The $Q_G(nP)$ values seem to saturate or even to slightly decrease, within experimental error.

(iii) For any given level the following inequalities hold:

$$Q_{Rb} \gg Q_{He} > Q_{Ar} > Q_{Ne}.$$

Before discussing these results, we would first like to point out that knowledge of the nature of the end products for the quenching process would be of great help for developing experiments concerning the collisional properties of Rydberg states and for the elaboration of theoretical treatments concerning these processes. We wish, therefore, to consider the various processes responsible for the quenching of a highly excited nP state and their relative efficiencies. Two different types of mechanism are involved: (a) The first mechanism leads to neutral end products [the neutral channels of reaction (1)]. There is a transfer of electronic excitation from the nP state to other rubidium bound states. (b) The second mechanism leads, when energetically possible, to ionic end products [the ionic channels of reaction (1)].

We shall show that the second mechanism can be considered as negligible with respect to the first one, under the present experimental conditions.

Consider first the direct ionization process:

$$\mathrm{Rb}(nP) + X \rightarrow \mathrm{Rb}^+ + X + e^-, \quad (5)$$

where X is a ground-state rubidium or rare-gas atom. Reaction (5) is energetically possible for $n \geq 19$ if one considers a collision occurring with the relative velocity of the reactants equal to the Maxwellian averaged velocity. A recent theoretical work[13] has shown that the cross section σ_i for reaction (5) is always less than the cross section σ for a free electron elastically scattered by atom X. Equation (9) of Ref. 13 gives $\sigma_i = \sigma\phi(\chi)$, where $\phi(\chi) = 2.5\chi^3$. The parameter χ (roughly the ratio of the atomic velocity of rubidium and X atoms to the valence electron velocity in its nP orbit) is of the order of 10^{-2} for the present experimental conditions. Considering the values of the elastic cross section σ,[14,15] which are about one order of magnitude smaller than the cross sections $Q_X(nP)$ reported here, the contribution of reaction (5) to the total quenching can therefore be regarded as completely negligible.

Lee and Mahan[16] have shown that, for the levels considered in this study ($12 \leq n \leq 22$), the two following reactions, leading to ionic end products, are present in a pure rubidium vapor:

$$\mathrm{Rb}(nP) + \mathrm{Rb}(5S) \rightarrow \mathrm{Rb}_2^+ + e^- \quad \text{(associative ionization)}, \quad (6)$$

$$\mathrm{Rb}(nP) + \mathrm{Rb}(5S) \rightarrow \mathrm{Rb}^+ + \mathrm{Rb}^-. \quad (7)$$

The values of the corresponding cross sections have not been measured, but the results indicate that the two reactions have comparable efficiencies. Experimental studies[17] recently have shown that the associative ionization cross sections are about 10^{-15} cm^2 for $n \sim 10$–12 in the case of the cesium nP levels. Assuming for the $12P$ level of rubidium an associative ionization cross section on the same order of magnitude, it can be concluded that processes (6) and (7) contribute negligibly to the collisional depopulation of this level, since the corresponding cross section for this process is 2.3×10^{-13} cm^2. The same conclusion should also hold for the highest level ($22P$) investigated here in view of the behavior of the associative ionization cross sections as a function of n. Thus the quenching reactions leading to neutral products seem to be more efficient than those leading to ionic products in the case of Rb-Rb collisions.

As far as we know, there is no information concerning the efficiency of the reaction:

$$\mathrm{Rb}(nP) + G \rightarrow (\mathrm{Rb}^+ - G) + e^-, \quad (8)$$

where G is a ground-state rare-gas atom. Considering the theoretical potential curves for the

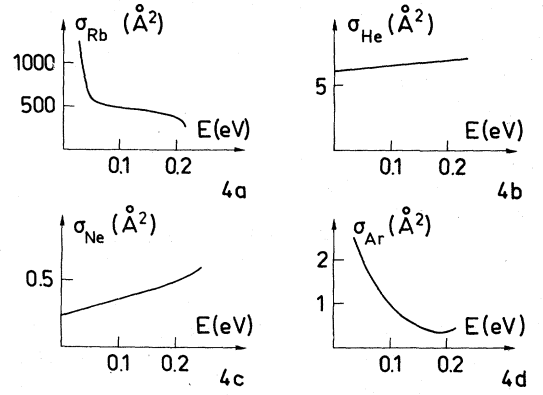

FIG. 4. Electron-atom elastic scattering cross sections vs electron energy E for Rb(4a), He(4b), Ne(4c) and Ar(4d).

(Rb^+-G) ionic complex[18] and the Maxwellian averaged relative velocity of the two colliding atoms, it seems that this ionic channel is energetically accessible when $n \geq 19$ for Rb-He and Rb-Ne collisions and when $n \geq 15$ for Rb-Ar collisions. Because the $Q_{He,Ne,Ar}(nP)$ quenching cross-section values show no apparent discontinuity when going from the $14P$ to the $22P$ level, one may conclude that process (8) gives a small or negligible contribution to the collisional quenching of the considered nP levels.

To summarize, we believe that the ionic channels represent only a minor contribution to the depopulation of the highly excited nP states and that the depopulation is therefore due mainly to excitation transfer to neutral atomic states. We arrived at the same conclusion in a previous work[3] concerning the total quenching cross section of the $10P$ level of potassium, in which we showed that several neighboring levels were noticeably populated under similar experimental conditions.

The outer electron of an alkali atom lying in a Rydberg state is very weakly bound (the average orbit radius is about 10^2 Å), and only its velocity distribution, which is non-Maxwellian, accounts for the discrete character of the energy spectrum. This quasifree behavior is often discussed in the literature and is the basis of most of the theoretical works on Rydberg states. Recently such a theoretical approach[5] has led to an excellent agreement with experimental results[2] concerning collisions of highly excited F states of xenon atoms and SF_6 molecules and the subsequent formation of SF_6^- and Xe^+ ions. However, no systematic evidence of this quasifree behavior of the outer electron has been demonstrated for atom-atom collisions. It is interesting to see now if our results can be explained using this argument, i.e., how elastic rate constants for free-electron noble gas (or rubidium) scattering compare with the quenching rate constants deduced from our measurements. For this comparison to be of some value, however, it is necessary that the change in potential energy resulting from the quenching process is small compared with the collision energy. For a collision energy of about 410 cm^{-1}, only the $22P$ level fulfills this requirement, since the potential energy change corresponding to a transition to the $21D$ level is $+9$ cm^{-1} and to the $19F$ level is -10 cm^{-1}. We thus restrict the comparison to this case.

Figure 4 shows the well established (e^--rare gas) elastic scattering cross sections,[14] as a function of energy in the range of interest, and the (e^--rubidium) elastic scattering cross section for which few reliable quantitative results are available.[15] In the latter case a rapid increase of the cross section is observed with decreasing energy. In Table II we compare the Maxwellian averaged rate constants $K_X^Q(22P)$ [deduced from our measurements; see Eq. (2)] and the corresponding electron scattering rate constants $K_X^e(22P)$ which are derived from

$$K_X^e(22P) = \int_0^\infty v\sigma_x(v) f(v)\, dv\,, \tag{9}$$

where $\sigma_x(v)$ is the elastic scattering cross section and $f(v)$ the relative velocity distribution[19] of the outer electron for the $22P$ level considered. The comparison shows that the $K_X^e(22P)$ values exhibit the qualitative features (i) and (iii) mentioned at the beginning of this section, although the absolute values of $K_X^e(22P)$ and $K_X^Q(22P)$ noticeably differ (from a factor of 3 to 20). Even for the highest level investigated here, the changes in potential energy resulting from the quenching process ($+9$ and -10 cm^{-1}) are too large to allow a reliable treatment in terms of elastic scattering.

In Table III we report the values of the quenching rate constants $K_{He}^{BE}(nP)$ obtained for the helium case from the binary-encounter theory for atom-atom inelastic collisions developed by Flannery.[6] In this theoretical approach, (a) the elastic scattering of the outer electron by the perturbing atom is taken into account, (b) the e^--alkali core Cou-

TABLE II. Quenching rate constants K_X^Q and valence electron-atom elastic rate constants K_X^e for the $22P$ state of rubidium. All values are in $cm^3\,sec^{-1}$.

Perturber X	K_X^Q	K_X^e
Rb	7.6×10^{-8}	77×10^{-8}
He	9.7×10^{-10}	40×10^{-10}
Ne	1.01×10^{-10}	3.3×10^{-10}
Ar	1.8×10^{-10}	36×10^{-10}

TABLE III. Quenching rate constants K_{He}^{Q} and binary-encounter rate constants K_{He}^{BE} for Rb-He collisions. All values are in $cm^3\ sec^{-1}$.

Level	K_{He}^{Q}	K_{He}^{BE}
12P	6.0×10^{-10}	27×10^{-10}
14P	8.9×10^{-10}	41×10^{-10}
17P	9.2×10^{-10}	64×10^{-10}
22P	9.7×10^{-10}	88×10^{-10}

lombic interaction is used to determine the velocity distribution of the valence electron, (c) the interaction between the alkali core and the perturbing atom is ignored, and (d) the inelastic collision is treated by classical mechanics.

Flannery has used this approach to study collisions between excited ($n \geq 10$) and ground-state hydrogen atoms at thermal energies. We have calculated, according to Ref. 6, the rate coefficient K_{He}^{BE} by summing the rate coefficients associated with the various inelastic processes which give noticeable contributions to the K_{He}^{BE} values. We have considered the helium case because the (e^--He) elastic cross section can effectively be taken as a constant [see Fig. 4(b)] thereby simplifying the calculations. The calculated rate constants K_{He}^{BE} and the K_{He}^{Q} values vary the same way with n, but the K_{He}^{BE} values are always larger than the experimental ones by a factor between 4.5 and 9.

It appears that a simple two-body theory, involving only the alkali valence electron and the perturbing atom is unable to correctly reproduce the present experimental results. [The large cross sections obtained for the Rb(nP)-Rb(5S) collisions may be partly due to the fact that the reactants are of identical atomic species.] Therefore, the alkali core should also be considered in the theoretical treatment of the collision problem. This has also been recently pointed out by Smirnov[20] following his study of the quenching of highly excited hydrogen atoms by ground-state helium atoms. A theory based on a three-body interaction model, involving the alkali core, the valence electron, and the perturbing atom is expected to yield a better agreement with the present experimental results. In particular, a formulation of the collision problem in terms of adiabatic potentials of the alkali-perturbing atom system seems to be well suited to the study of these collisions at thermal energies.

The only previous experimental works dealing with atom-atom collisions involving Rydberg states are those of Gallagher *et al.*,[1,21] who have studied the collisional angular momentum mixing of highly excited nD states ($6 \leq n \leq 15$) in sodium induced by collisions with rare gases, that is to say the transfer of electronic excitation of the ($n; l = 2$) state towards the group of neighboring levels ($n; l > 2$). For this particular process (which represents, as pointed out by Gallagher *et al.*,[1] the major part of the collisional quenching of the nD states) very high cross-section values (of the order of 10^{-13} cm^2) have been measured. The cross sections are found to rise rapidly with increasing n to a maximum at $n = 10$ and from there to decrease slightly for higher n values. A similar behavior of our quenching cross sections for increasing values of n was observed, although they are one to two orders of magnitude lower than those reported by Gallagher *et al.*, and refer to a different collisional process. One has to be careful when comparing the two experiments because the investigated levels occupy quite different positions in their respective energy diagram. The nD states of sodium investigated by Gallagher *et al.* are very close to the ($n; l > 2$) states (the energy defect is less than 1 cm^{-1} for $n \sim 12$) but are well isolated from the other states. In contrast the nP states of rubidium are well isolated from all the other states (at least 9 cm^{-1} for $n = 22$). Thus one might expect the collisional quenching cross sections of the nP Rb states to be lower than those of the corresponding nD states for the Na atoms. Our results and those of Gallagher *et al.* are therefore not at all contradictory. In other words the order of magnitude difference between the results of the two experiments may be due in part to the fact that electronic transition in Na–rare-gas collisions take place at internuclear distances much larger than for the Rb–rare-gas collisions.

Table IV shows the rate coefficients K_{He}^{Ga} deduced from the experimental results of Gallagher *et al.*[21] in the case of helium and the rate coefficients K_{He}^{e} calculated according to Eq. (9)(the scattering of

TABLE IV. Experimental rate constants K^{Ga} for the collisional angular momentum mixing of highly excited D states of sodium in collision with helium (results of Gallagher *et al.*, see Ref. 21). K^e is deduced from Eq. (9) (see text), K_{He}^{Ol} from Ref. 23. All values are in $cm^3\ sec^{-1}$.

Level	K_{He}^{Ga}	K_{He}^{e}	K_{He}^{Ol}
6D	5.7×10^{-9}	2.0×10^{-8}	1.0×10^{-8}
7D	1.2×10^{-8}	1.8×10^{-8}	3.4×10^{-8}
8D	1.6×10^{-8}	1.5×10^{-8}	2.9×10^{-8}
9D	1.6×10^{-8}	1.3×10^{-8}	1.7×10^{-8}
10D	3.3×10^{-8}	1.2×10^{-8}	1.5×10^{-8}
11D	2.8×10^{-8}	1.1×10^{-8}	1.3×10^{-8}
12D	2.5×10^{-8}	1.0×10^{-8}	1.2×10^{-8}
13D	2.5×10^{-8}	9.3×10^{-9}	1.2×10^{-8}
14D	2.0×10^{-8}	8.6×10^{-9}	1.1×10^{-8}
15D	2.0×10^{-8}	8.1×10^{-9}	1.1×10^{-8}

the quasifree electron on the helium atom). It is seen that for $n \geq 8$ these rate coefficients are in agreement within a factor B, $1 \leq B \leq 3$, better than the similar comparison for the Rb-He collision (see Table II). This is not surprising in view of the potential energy changes involved in the angular momentum mixing process studied by Gallagher *et al.* A recent two-state quantum mechanical calculation by Olson[22,23] using asymptotic adiabatic potential curves for the Na–rare-gas systems is in reasonable agreement with all the experimental results of Gallagher *et al.* (see Table IV where only Na-He results are reported). It is interesting to note that the rate constants K^e_{He} for Na(nD)-He collisions agree within 30% with the corresponding rate constants K^{ol}_{He} deduced from the theoretical values obtained by Olson for $n>8$. For heavier rare gases, elastic rate constants compare less satisfactory with experimental and Olson values. This reflects the growing importance of both the polarization effects (Van der Waals interaction) and the electron–rare-gas exchange interaction with increasing mass of the rare gas, the latter being significant even at large internuclear distances.[24]

V. CONCLUSION

Collisional quenching cross sections of highly excited nP states of rubidium ($12 \leq n \leq 22$) have been measured at thermal energies as a function of n and the nature of the perturbing atom. It is observed that the cross-section values do not increase with n as the geometrical size of the excited atom (i.e., as n^4). In particular the cross sections for Rb–rare-gas collisions seem to reach a constant value or even to slightly decrease.

The quenching of these nP states has been shown to be mainly due to electronic excitation transfer to neighboring atomic levels. In view of the fact that these levels are close in energy to the nP states we find the Rb–rare-gas cross-section values surprisingly small.

No simple model, i.e., a two-body model taking into account only the interaction of the quasifree valence electron with the perturbing atom, can explain in a satisfactory way our experimental results. The Rb–rare-gas quenching processes occur at internuclear distances for which a theoretical calculation must apparently make use of adiabatic potential curves derived from a three-body model (valence electron, core of Rb, perturbing atom). For some processes having large cross sections a simpler approach using asymptotic potentials may lead to a satisfactory agreement with experiment.

ACKNOWLEDGMENTS

We acknowledge the help of J. Cuvellier during the measurements and are indebted to M. Ahrweiller and J. P. Felix for developing and building the acquisition system. We would like to thank J. Pascale for helpful discussions and valuable comments, and T. F. Gallagher for providing his data prior to publication. We wish to thank L. Pitchford and R. A. Gutcheck for carefully reading the manuscript.

[1] T. F. Gallagher, S. A. Edelstein, and R. M. Hill, Phys. Rev. Lett. 35, 644 (1975).
[2] W. P. West, G. W. Foltz, F. B. Dunning, C. J. Latimer, and R. F. Stebbings, Phys. Rev. Lett. 36, 854 (1975).
[3] F. Gounand, J. Cuvellier, P. R. Fournier, and J. Berlande, J. Phys. (Paris) 37, L169 (1976).
[4] I. C. Percival and D. Richards, Adv. At. Mol. Phys. 11, 1 (1975).
[5] M. Matsuzawa, J. Phys. Soc. Jpn. 32, 1088 (1972).
[6] M. R. Flannery, Ann. Phys. (N.Y.) 61, 465 (1970).
[7] A. N. Nesmeyanov, *Vapor pressure of the elements* (Academic, New York, 1963).
[8] F. Gounand, P. R. Fournier, J. Cuvellier, and J. Berlande, Phys. Lett. 59A, 23 (1976).
[9] E. M. Anderson and V. A. Zilitis, Opt. Spektrosk. 16, 382 (1964) [Opt. Spectrosc. 16, 211 (1964)].
[10] See for example, J. S. Deech, R. Luypaert, and G. W. Series, J. Phys. B 8, 1406 (1975).
[11] M. Gross, C. Fabre, P. Pillet, and S. Haroche, Phys. Rev. Lett. 36, 1035 (1976).
[12] A. Gallagher and E. L. Lewis, J. Opt. Soc. Am. 63, 864 (1973).
[13] B. M. Smirnov, *Invited lectures, review papers, and progress reports of the Ninth International Conference on the Physics of Electronic and Atomic Collisions*, edited by T. S. Risley and R. Geballe (University of Washington Press, 1975), p. 701.
[14] H. S. W. Massey, *Electronic and Ionic Impact Phenomena* (Oxford, New York, 1969), Vol. 1, Chap. 6. See also D. E. Golden and H. W. Bandel, Phys. Rev. 149, 58 (1966); and C. Sol, F. Devos, and J. C. Gauthier, Phys. Rev, A 12, 502 (1975).
[15] L. C. Balling, Phys. Rev. 179, 78 (1968). A more recent calculation by I. I. Fabrikant [Phys. Lett. 58A, 21 (1976)] indicates cross section about 50% higher than those calculated by Balling. This discrepancy is not important for the purpose of this work.
[16] Y. T. Lee and B. H. Mahan, J. Chem. Phys. 42, 2893 (1965).
[17] E. E. Antonov, Y. P. Korchevoy, V. I. Lukashenko, and I. N. Hilko, *Proceedings of the Twelfth International Conference on Ionization Phenomena in Gases*, p. 33, Eindhoven, 1975, edited by J. G. A. Hölschen and D. C. Schram, (North Holland, American Elsevier, Amsterdam, 1975).
[18] J. Pascale (private communication).
[19] B. Podolsky and L. Pauling, Phys. Rev. 34, 109 (1929).
[20] V. A. Smirnov, Opt. Spektrosk. 37, 407 (1974) [Opt.

Spectrosc. 37, 231 (1974)].
[21]T. F. Gallagher, S. A. Edelstein, and R. M. Hill, Phys. Rev. A 15, 1945 (1977).
[22]S. A. Edelstein, T. F. Gallagher, R. E. Olson, and R. M. Hill, *Abstracts of the Fifth International Conference on Atomic Physics*, edited by R. Marrus, M. H. Prior, and H. A. Shugart (Berkeley, 1976), p. 240.
[23]R. E. Olson, Phys. Rev. A 15, 631 (1977).
[24]The adiabatic potential curves for the alkali-helium systems are rather flat. J. Pascale and J. Vandeplanque, J. Chem. Phys. 60, 2278 (1974). See also J. Pascale and J. Vandeplanque, CEA Report (unpublished), available on request from the authors. The curves for the other alkali–rare gas systems exhibit a structure which becomes more pronounced with increasing mass of the rare-gas atom.